

NW-CENTRAL SOUTH POLE-AITKEN: COMPOSITIONAL DIVERSITY, GEOLOGIC CONTEXT, AND IMPLICATIONS FOR BASIN EVOLUTION. D. P. Moriarty¹, P. J. Isaacson², and C. M. Pieters¹, ¹Dept. Geol. Sci., Brown Univ., Providence RI, ²HIGP, Univ. of Hawaii, Manoa HI.

Introduction: The South Pole-Aitken Basin (SPA) on the lunar farside is one of the largest impact basins in the solar system and provides key constraints for the understanding of basin impact processes, lunar impact history, and the compositional structure of the lunar crust. VIS-NIR spectroscopy of surficial materials and central peaks reveal the non-mare SPA interior to be rich in low-Ca pyroxene (LCP) [1,2,3,4,5,6]. This LCP-bearing material may be derived from the lower crust or a large melt sheet incorporating lower crust and mantle material [1,2,4,7]. Additional information for basin stratigraphy include Mg# differences in LCPs [8] and the possible identifications of olivine [9] and anorthosite [1,9,10] in certain regions. Characterizing the stratigraphy and spatial distribution of materials in the basin provide fundamental constraints.

Data and Methods: Here, Moon Mineralogy Mapper (M³) hyperspectral data are used to investigate a region in NW SPA including Leibnitz (245 km), Finsen (72 km) and Davisson (87 km), shown in Fig. 1c. Continuum removal and spectral parameters described in [6] are used to characterize the spatial distribution of distinct lithologies in the region. Key parameters include estimated band center (EBC) and band depth (BD) for the 1 μ m mafic absorption, both obtained through parabola fitting. Since band center is sensitive to mineralogy and chemistry and band depth is sensitive to mafic abundance, these parameters provides a good compositional overview.

Variations in band center (x-axis) and band depth (y-axis) values for each pixel in the image are shown on a scatterplot (Fig. 1a+b). Soils dominate the central portion of the scatterplot, but this approach allows distinct compositions and mixing trends to be identified. Pixels on the scatterplot with similar

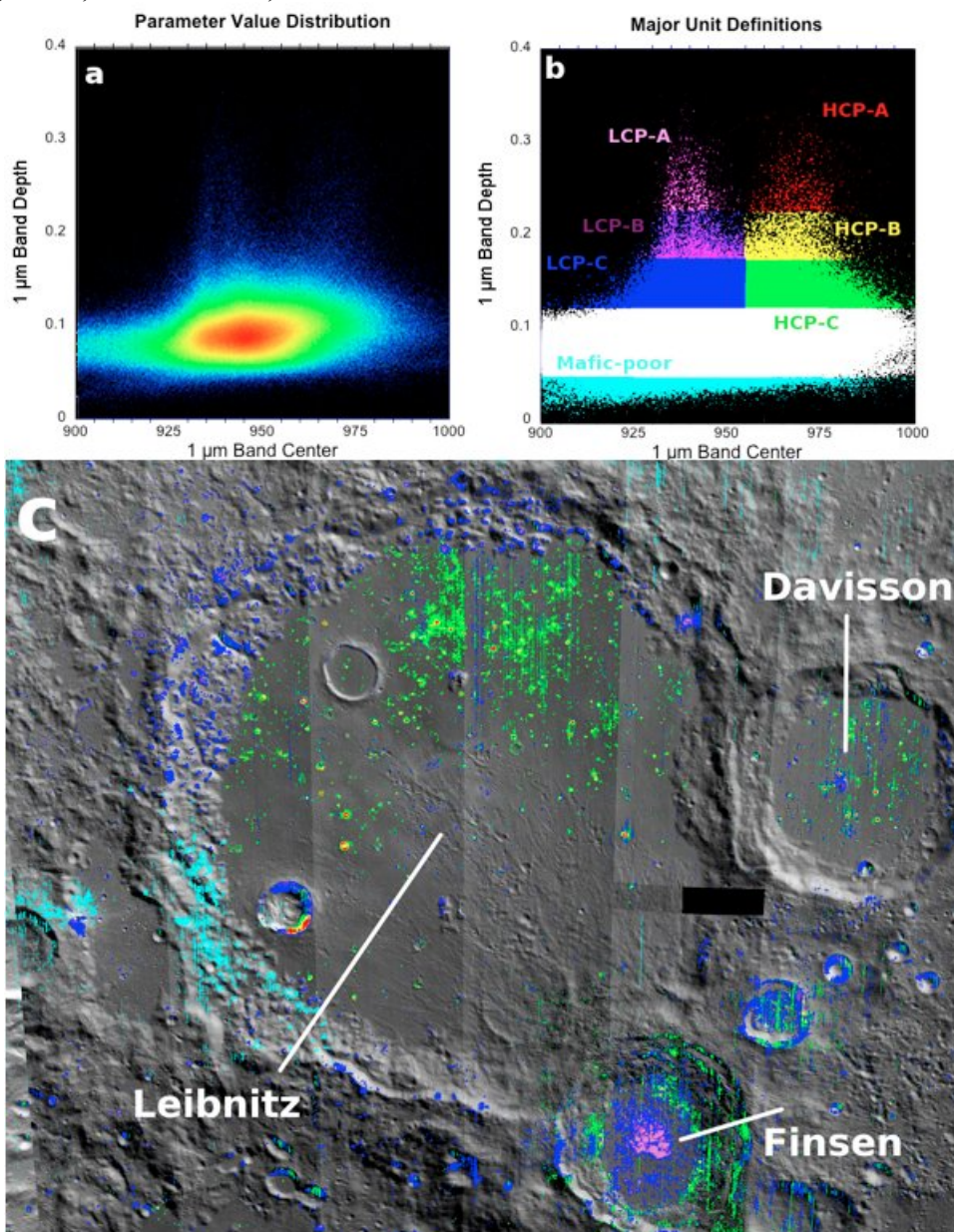


Fig. 1: (a) Distribution of EBC (x-axis) and BD (y-axis) values for each pixel in the Leibnitz region. Red indicates the highest pixel density and is associated with soils. (b) Pixels sharing similar parameter values are assigned colors to highlight distinct lithologies and mixing trends. (c) Each colored pixel from (b) is shown on the map of the Leibnitz region to investigate the spatial distribution of the observed lithologies.

parameter values are highlighted in the M³ image to investigate the spatial distribution of each lithology.

Results: At least three distinct lithologies (plus soils) are apparent across this region: Low-Ca pyroxene (LCP) -bearing, high-Ca pyroxene (HCP) -bearing, and mafic-poor. The spatial distributions for

each lithology are presented in Fig. 1c. Average spectra of each unit are given in Fig. 2.

LCP-bearing. In Fig. 1b, the LCP unit ($BD > 0.125$, $EBC < 960$ nm) is highlighted blue-violet on the map. The strongest absorption bands are present in Finsen's central peak, but also appear interspersed with weaker bands in Leibnitz's wall, Davisson's central peak, and smaller craters. Mixing or weathering trends are apparent in band strength variations. Spectra of LCP-bearing materials from Leibnitz's wall appear similar in band center and shape to spectra of Finsen's central peak.

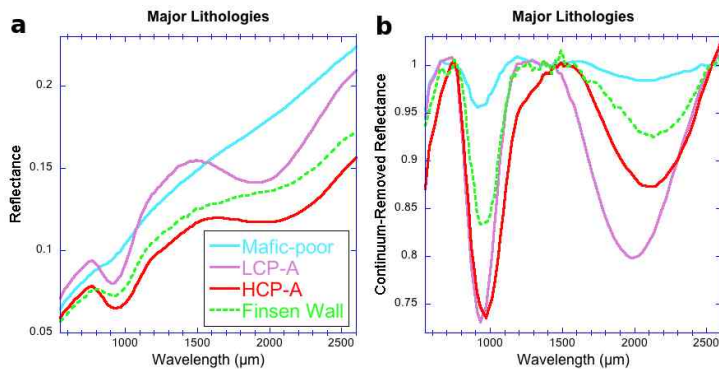


Fig. 2: (a) Mean reflectance spectra of the mafic-poor, LCP-A, and HCP-A units defined in Fig. 1b. An average spectrum from the HCP-bearing material in Finsen's wall is included for comparison. (b) Continuum-removed reflectance for the same areas.

HCP-bearing. In Fig. 1b, the HCP-bearing unit ($BD > 0.125$, $EBC > 960$ nm) is highlighted green-red on the map. The strongest absorption bands are apparent in small mare craters in Leibnitz and Davisson. HCP-bearing materials are also present in Finsen's wall and ejecta. However, as shown in Fig. 2, spectra of Leibnitz's mare display a wider shoulder at ~ 1.2 μ m than spectra of Finsen's wall.

Mafic-poor. In Fig. 1b, the mafic-poor unit ($BD < 0.05$) is highlighted cyan on the map. The mean spectrum of this unit in Fig. 3 exhibits very weak mafic bands and a subtle 1.25 μ m band, indicating the presence of abundant crystalline plagioclase. Extensive exposures of mafic-poor materials occur in the SW rim and ejecta of Leibnitz.

Discussion: Significant compositional diversity is observed in the Leibnitz-Finsen region. Stratigraphic relationships between lithologies are derived from superposition relations and the relative size of post-SPA craters.

A melt sheet formed by the SPA impact is likely composed of lower crust or upper mantle material and may be highly mafic [1,13]. However, the presence of extensive mafic-poor materials in Leibnitz's SW wall and ejecta suggests that Leibnitz has exhumed upper crustal material, perhaps buried beneath a thin layer of

impact melt. Although the mafic-poor material may place a lateral constraint on the extent of the SPA melt sheet, the prominent LCP-rich lithology of Finsen's central peak may indicate a transition to a thicker layer of impact melt toward the center of the basin.

HCP-rich materials appear confined to surficial or shallow layers. Most of these materials are present in the form of surficial mare deposits. The HCP-bearing materials observed in Finsen are an exception. These materials (observed in Finsen's wall and ejecta) are derived from a shallower source region than the LCP-rich central peak (which is likely derived from ~ 10 km [14]). The origin of HCP-bearing material in Finsen is unknown, but the difference in spectral character compared to mare basalts in Leibnitz suggests a separate source, perhaps with a different cooling history [11,12]. For example, the HCP-bearing material in Finsen could be from a feeder dike that stalled and pooled below the surface, cooling slowly. Since Finsen (Eratosthenian) was formed after the formation of Leibnitz (Pre-Nectarian) and subsequent mare volcanism (most active during the Imbrian) [15,16], it would have excavated any near-surface intrusive emplacements present.

Conclusions and future work: The spectral processing tools developed and used here effectively identify and map distinct lithologies in M^3 data. Using these tools, compositional diversity and stratigraphic relationships are observed in the NW-central region of SPA. The LCP-rich materials observed in the central peaks of Finsen are likely derived from the SPA melt sheet. Extensive mafic-poor materials exposed by Leibnitz place vertical or lateral constraints on the extent of the mafic melt sheet. Finsen's wall and ejecta may have also excavated an undifferentiated intrusive body similar in composition to the mare basalts in Leibnitz. These tools for compositional assessment will be applied to other areas of SPA to continue characterizing the basin interior and stratigraphy.

Acknowledgements: This analysis is supported through NASA NLSI grant NNA09DB34A.

References: [1] Pieters C. M. et al. (2001) *JGR*, 106, E11, 28,001-28,022. [2] Pieters C. M. et al. (1997) *GRL*, 24, 1903-1906. [3] Tompkins S. and Pieters C. M. (1999) *Met. & Planet. Sci.*, 34, 25-41. [4] Nakamura, R. et al. (2009) *GRL*, 36, L2202. [5] Cahill J. T. et al. (2009) *JGR*, 114, E09001. [6] Moriarty D. M. et al. (in preparation). [7] Morrison D. A. (1998) *LPSC XXIX*, #1657. [8] Klima R. L. et al. (2011) *JGR*, 116, E00G06. [9] Yamamoto S. R. et al. (2012) *Icarus*, 218, 331-344. [10] Ohtake M. et al. (2009) *Nature*, 461, 236-241. [11] Klima R. L. et al. (2007) *Met. & Planet. Sci.*, 42, 235-353. [12] Klima R. L. et al. (2011) *Met. & Planet. Sci.*, 46, 379-395. [13] Lucey P. G. et al. (1998) *JGR*, 103, 3701-3708. [14] Cintala M. J. and Grieve R. A. F. (1998) *Met. & Planet. Sci.*, 33, 889-912. [15] Wilhelms D. E. et al. (1987), *USGS, 1348*. [16] Head J. W. (1976) *Rev. Geophys. Space Phys.*, 14, 265-300.